PHYSICAL REVIEW B VOLUME 51, NUMBER 6 1 FEBRUARY 1995-II

Quantum tunneling in solid D_2 and solid H_2

Erika G. Kisvarsanyi and N. S. Sullivan
Department of Physics, University of Florida, Gainesville, Florida 32611

(Received 19 August 1994)

We report calculations of quantum tunneling in solid deuterium and solid hydrogen using a most-probable-escape-path method for tunneling in quantum crystals. We estimate the rates for tunneling by quantum-mechanical exchange in solid H_2 and D_2 and calculate specifically the tunneling of HD impurities and paradeuterium impurities in solid parahydrogen and solid orthodeuterium. These calculations are compared with the results of recent experiments.

I. INTRODUCTION

The quantum crystals (solid hydrogens and solid heliums) are unique among solids in that the atoms or molecules are only weakly localized about their equilibrium lattice sites. The root-mean-square displacement associated with this zero-point motion is 35% of the lattice spacing in solid ^{3}He (at the highest molar volume) and 18% in solid H_2. The single-particle wave functions overlap appreciably and this leads to particle-particle quantum-mechanical exchange between neighboring sites. This exchange is well known and well understood for solid ^{3}He,[1–3] where 2, 3, 4, or more atoms may be involved in a cyclic exchange at rates as high as 30 MHz at the highest molar volume. This high exchange rate leads to a motional narrowing of the cw NMR line shape by several orders of magnitude, and is responsible for the onset of nuclear antiferromagnetism at 1.9 mK.

Exchange rates of this magnitude are not expected to occur in solid H_2 because of the reduced zero-point energy and stronger localization of the molecules at the lattice sites. Quantum-mechanical particle-particle exchange is nevertheless predicted theoretically for solid H_2,[4] the only question being whether the exchange rates are sufficiently high to be observable. Early modes of exchange that only allowed for two particle exchange[4] predicted rates as low as 10^{-2}–10^{-4} Hz which were not expected to be observable. However, more recent models[3] that include multiparticle exchange lead to rates as high as 10^2–10^4 Hz, and these rates would certainly lead to observable effects.

Experiments have been carried out to test for the existence of particle-particle tunneling in solid H_2. These have involved NMR studies of HD impurities in a matrix of almost pure para-H_2.[5,6] Both HD molecules and the para-H_2 molecules are in their ground states (angular momentum $J=0$), and motional effects can only be attributed to particle-particle tunneling.[7] This tunneling process involving mass transfer is to be distinguished from the so-called resonant conversion process. In this case, there is an exchange of angular momentum quantum numbers between a $J=1$ molecule at one lattice site and a $J=0$ molecule at another site resulting in the quantum diffusion of a $J=1$ impurity in a $J=0$ matrix.

This diffusion of angular momentum occurs as a result of the nuclear magnetic dipole-dipole interactions between the molecules.[8,9] The magnetic interactions are also responsible for the familiar ortho-to-para conversion that leads to the decay of the metastable $J=1$ states to the $J=0$ ground states in H_2 and D_2.[10] For this reason, the quantum diffusion process in which a $J=1$ particle at one site and a $J=0$ particle at another site exchange angular momenta is referred to as "resonant conversion." Both processes occur simultaneously for $J=1$ impurities in a $J=0$ H_2 matrix, but *only* exchange tunneling (mass transfer) can occur for HD particles in a $J=0$ para-H_2 matrix because the HD molecules are also in a $J=0$ state.

Two different types of NMR studies of HD impurities have been carried out: (1) cw NMR studies[5] which show a narrow HD line shape smaller than the calculated rigid lattice line shape (Fig. 1), and (2) pulsed studies[5,6] to determine the nuclear spin-spin relaxation time T_2 and the nuclear spin-lattice relaxation time T_1. The apparently motionally narrowed cw line is consistent with the relative width of echoes in pulse studies.[6] The earliest studies of T_2 (Ref. 11) used rather long-rf-pulse techniques that did not cover the full width of the ortho-H_2 ($J=1$) impurity line shape. Although values of T_2

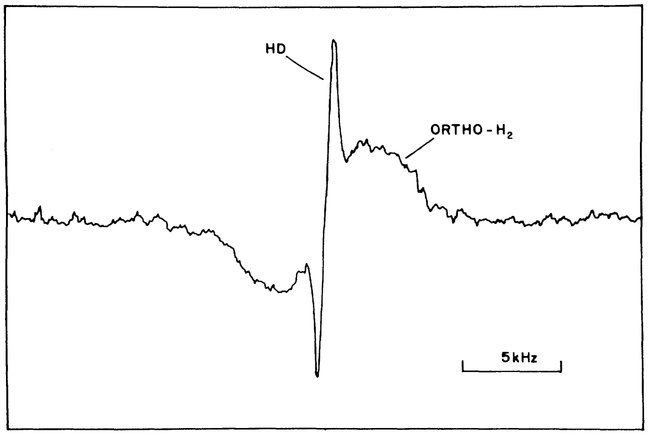

FIG. 1. Derivative NMR line shape for HD impurities (1.1%) in solid para-H_2 with 1.8% ortho-H_2 impurities, showing the motional narrowing of the HD line shape.

0163-1829/95/51(6)/3462(7)/$06.00

longer than the rigid lattice values were observed, the results could be attributed to the long rf pulse techniques used.[12] Subsequent studies using high power short rf pulses,[6] however, also showed that the T_2 values were longer than the rigid lattice values and were consistent with the cw measurements. The cw line shapes at low temperatures and the values of T_2 determined from high power pulsed techniques were interpreted in terms of an effective particle-particle exchange rate of approximately 1 kHz.[6] Analyses of the spin-lattice relaxation rates[13] also supported this interpretation.

The interpretation of the NMR results for HD impurities in para-H_2 in terms of particle-particle exchange has, however, had to be reexamined because of the small pressure dependence observed for the low temperature T_2 values.[14] The exchange rates, J_3, in solid ^{3}He are observed to be strongly dependent on the molar volume, $J_3 \sim V^{19}$. A similar dependence is expected to be valid for solid H_2 (Ref. 3) if the exchange rates are largely determined by geometrical considerations, i.e., the available free volume for exchange. Application of pressures of about 100 bar were predicted to reduce the exchange rates in H_2 by almost two orders of magnitude and thus reduce T_2 to the rigid lattice values.[3] This was not observed experimentally.[14] Application of a hydrostatic pressure of 136 bar reduced T_2 from 3.4 msec to only 2.5 msec, compared to a calculated rigid lattice value of 0.5 msec. There are two unanswered questions concerning this result. First, why was the limiting value of 2.5 msec for T_2 still very large compared to the rigid lattice value and, second, if there is no motion, how does one understand a 20% reduction of T_2 when the $\langle R^{-6} \rangle$ dependence for a rigid lattice is only 2% for this pressure change? This suggests that motional effects are relevant but that the mechanism for the increase of T_2 over the rigid lattice value is not well understood. A quantitative understanding of the pressure dependence has not been attained.

In order to obtain an independent test for the possibility of quantum-mechanical tunneling in the solid hydrogens, Krivchikov *et al.*[15] have studied the heat capacities of impurities of para-D_2 ($J=1$, 0.94%) and ortho-H_2 ($J=1$, 0.063%) in a para-H_2 ($J=0$) matrix. Because of the large difference in the rotational kinetic energies of the impurity $J=1$ D_2 molecules and the host $J=0$ H_2 molecules, $\Delta E_{\text{rot}}=85$ K (Fig. 2), quantum diffusion via the resonant conversion process (induced by nuclear magnetic interactions) is reduced by several orders of magnitude due to energy conservation at low temperatures. As a result, only particle-particle exchange tunneling is allowed.

The authors of Ref. 15 carried out a precise study of the time dependence of the peak at the heat capacity at 1.72 K to determine if tunneling occurs in this system. They observed a null result over a period of 290 h and concluded that the characteristic time constant for particle-particle exchange in this system was longer than 10^4 h. They viewed this as being in strong contradiction with the predictions of Ref. 3. The purpose of this article is to reexamine the predictions of Ref. 3 and to estimate the tunneling rate for $J=1$ para-D_2 impurities in a solid para-H_2 matrix.

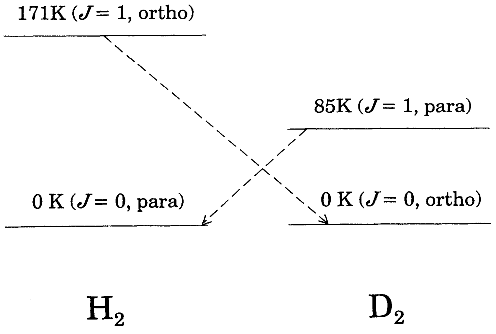

FIG. 2. Comparison of rotational kinetic energies for the conversion of a ($J=1$) para-D_2 molecule and with a ($J=1$) ortho-H_2 molecule.

There are two important local field effects to be considered in the calculation that significantly reduce the tunneling of $J=1$ para-D_2 in solid para-H_2: (a) the $J=1$ impurities have anisotropic interactions, and tunneling is reduced by conservation of energy requirements; (b) the H_2-D_2 mass difference leads to a crystal strain field around the D_2 impurity that must be dragged along in any tunneling process. The latter strain field results from the reduced zero point motion of the D_2 and the consequent contraction of the lattice around the D_2 impurity.

In order to calculate the effective tunneling rate for $J=1$ para-D_2 impurities we will use the value for tunneling inferred from NMR studies of HD impurities in para-H_2.[13] In Sec. III, we compare the predicted value with the experimental results of Krivchikov *et al.*[15] and show that observations of tunneling are not expected for the period covered in their experiments. We also calculate the tunneling rate for $J=1$ para-D_2 impurities in an ortho-D_2 ($J=0$) matrix and compare the results with the quantum diffusion observed in that system by Bagatskii *et al.*[16]

II. CALCULATION OF THE DIFFUSION OF $J=1$ IMPURITIES

The diffusion of angular momentum bearing ($J=1$) species can arise from either nuclear magnetic dipole-dipole interactions (as calculated by Van Kranendonk[17]) or by purely quantum-mechanical particle exchange (i.e., mass transfer). In this section, we first calculate the microscopic exchange, or tunneling, frequency resulting from quantum zero point motion. We then calculate the reduction of the tunneling frequency due to isotropic electrostatic quadrupole quadrupole (EQQ) interactions for $J=1$ impurities tunneling in a $J=0$ matrix.

An approximation for the tunneling rate must take into account the mass of the tunneling particle, and any interaction at the point of closest approach where the interaction is most relevant. In general, the tunneling frequency thus takes the form

$$\frac{\omega_t}{\omega_0} \approx \exp \int \sqrt{m V_{\text{eff}}}\, d\xi \;, \tag{1}$$

where ξ is a parameter characterizing the most probable escape path (MPEP) (Ref. 3) corresponding to the optimum trajectory for tunneling. V_{eff} is the effective interaction potential between particles and is dominated by the short-range repulsive interactions of close encounters during tunneling. It also accounts for the static elastic deformation surrounding the particles during the tunneling process. The mass of the tunneling particle is m, and ω_0 is a typical vibrational frequency.

In order to calculate the microscopic tunneling frequency of D_2 in a D_2 lattice, for example, we can use the following simple scaling relationship with H_2 because, in this case, only the mass changes (by a factor of 2). We have

$$\ln\left[\frac{\omega^{D_2/D_2}}{\omega_0}\right] = \sqrt{2}\ln\left[\frac{\omega^{H_2/H_2}}{\omega_0}\right] . \tag{2}$$

Using $\omega_0 = 2.64\times 10^{10}$ rad/sec (Ref. 18) and $\omega^{H_2/H_2} = 1$ kHz (Ref. 6) we find $\omega^{D_2/D_2} = 11.3$ rad/sec. (Note that we used the experimental values for HD tunneling in para-H_2 for ω^{H_2/H_2} and this could be an underestimation by a factor of about 5.)

The effective tunneling rate of the impurity, W_{eff}, is much less than this microscopic tunneling rate due to the anisotropic $J=1$ interactions as calculated by Van Kranendonk.[17] This can be easily understood if we consider energy conservation. A molecule can only tunnel from a given energy E_i at site i to an energy state E_j at site j if $|E_i - E_j| \le \hbar\omega$ where ω is the microscopic tunneling, or jump, frequency (Fig. 3). The tunneling rate is severely reduced because $\hbar\omega \ll \Delta$, the energy bandwidth due principally to quadrupolar interactions.

The jump frequency in a crystal for a single impurity tunneling from an initial state to a final state can be calculated as follows.[17] Defining the energy eigenvalues in the two states by

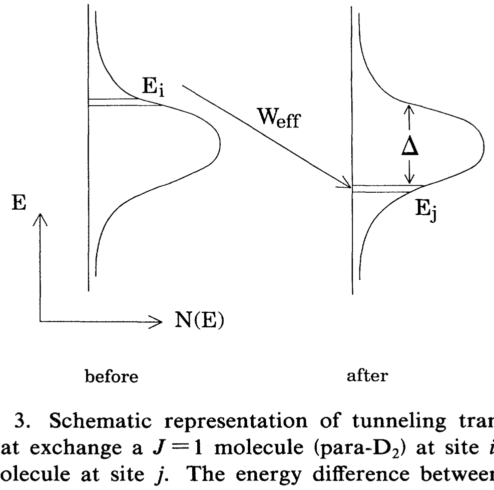

FIG. 3. Schematic representation of tunneling transitions. W_{eff} that exchange a $J=1$ molecule (para-D_2) at site i with a host molecule at site j. The energy difference between initial and final states, $E_i - E_j \ll \hbar\omega$, and the effective rate $W_{\text{eff}} \sim (\hbar\omega/\Delta)\omega \ll \omega$.

$$\hbar H|n_i\rangle = E_i|n_i\rangle, \quad \hbar H|n_j\rangle = E_j|n_j\rangle \;, \tag{3}$$

the jumping rate due to some perturbation V_{ij} can be written as

$$W = \frac{2\pi}{\hbar}\sum_{n_j} P_n |\langle n_j|V_{ij}|n_i\rangle|^2 \delta(E_j - E_i + \hbar\omega) \;, \tag{4}$$

where $\hbar\omega$ is the energy difference between the initial and final sites, and P_n is the Boltzmann factor. The δ function can be replaced by its Fourier time transform and using the energy eigenvalue equations, Eq. (3), can be rewritten as

$$W = \frac{1}{\hbar^2}\int_{-\infty}^{\infty} G(t) e^{i\omega t} dt \;. \tag{5}$$

The autocorrelation function $G(t) = \langle V(0)V(t)\rangle$, with the average taken over the distribution represented by the Boltzmann factor P_n, and $V(t) = e^{iHt}Ve^{-iHt}$.

For interactions between a statistical distribution of widely separated impurities, it is reasonable to assume that the correct final $G(t)$ can be characterized by a correlation time τ_Q,

$$G(t) = G(0) f\left[\frac{t}{\tau_Q}\right] \;, \tag{6}$$

and that a Gaussian form may also be assumed for the randomly distributed dilute system

$$G(t) = G(0) e^{-(1/2)(t/\tau_Q)^2} \;. \tag{7}$$

The correlation time τ_Q is the characteristic time scale of the autocorrelation function $G(t) = \langle V(0)V(t)\rangle$ and is therefore principally determined by the quadrupole-quadrupole interactions between the $J=1$ molecules, and possibly by anisotropic crystal fields at very low concentrations. The width of the energy bands of Fig. 3 is $\Delta \simeq \hbar\tau_Q^{-1}$. An average jump frequency must, therefore, be calculated over the energy distribution (Fig. 3) of impurities.[17] Noting that

$$G(0) = \frac{1}{N}\sum_{ij} |\langle n_j|V_{ij}|n_i\rangle|^2 \;, \tag{8}$$

we can determine $G(0)$ and thus W by evaluating the second moment of the EQQ interaction potential, V_{QQ},

$$M_2^{QQ} \equiv G(0) = \frac{1}{N}\sum_{ij} |\langle n_j|V_{QQ}|n_i\rangle|^2 \;. \tag{9}$$

The EQQ energy can be written as[19–21]

$$V_{QQ} = x^{5/3}\frac{\sqrt{70}}{R^5}Q^2 \sum_{|m|=0,2,4} \langle 2m, 2\bar{m}|40\rangle C_{2m}C_{2\bar{m}} \;, \tag{10}$$

where $\langle 2m, 2\bar{m}|40\rangle$ is the Clebsch-Gordon coefficient $C^{224}_{m\bar{m}0}$ and the C_{2m} are the Racah spherical harmonics. These Racah harmonics[22] are directly related (by a constant) to the spherical quadrupole tensorial operators T_{2m} (Ref. 23) which transform under rotations in the same manner as the spherical harmonics $Y_{2m}(\alpha,\beta)$. This formulation in terms of Racah harmonics is especially useful for calculating properties of solid H_2 (and D_2) such as nuclear spin relaxation rates.[23]

From Eq. (10), we find that

$$\langle V_{QQ}^2 \rangle = x^{10/3} \frac{70Q^2}{a_0^{10}} \left[\frac{1}{N} \sum_{ij} \left[\frac{a_0}{R_{ij}} \right]^{10} \right] \times \sum_{\pm m} |\langle 2m2\overline{m}|40\rangle|^2 \langle C_{2m} C_{2\overline{m}} (C_{2m} C_{2\overline{m}})^* \rangle \tag{11}$$

and finally,

$$\langle V_{QQ}^2 \rangle^{1/2} = \left[\frac{70}{9} \right]^{1/2} \Gamma x^{5/3} , \tag{12}$$

where $\Gamma = 6Q^2/25R^5$. Assuming the Gaussian form for $G(t)$, we have from Eq. (5)

$$W = \frac{1}{\hbar^2} \int_0^\infty G(0) e^{-(1/2)(t/\tau_Q)^2} e^{i\omega t} dt \tag{13a}$$

$$= \frac{\sqrt{2\pi}}{\hbar^2} G(0) \tau_Q e^{-(1/2)\omega^2 \tau_Q^2} . \tag{13b}$$

Defining the average jump frequency as $\omega = \sqrt{G(0)/\hbar^2}$, we find for the effective jump frequency

$$W_{\text{eff}} = \sqrt{2\pi}\omega^2 \tau_Q e^{-(1/2)\omega^2 \tau_Q^3} . \tag{14}$$

While ω is known from the above microscopic calculation, values for τ_Q for solid H_2 have already been calculated by Van Kranendonk.[17] Since $\omega\tau_Q \ll 1$, we find

$$W_{\text{eff}} = \sqrt{2\pi}\omega^2 \tau_Q . \tag{15}$$

Using the value $\omega^{D_2/D_2} = 11.3$ rad/sec for the microscopic tunneling frequency as calculated earlier, and $\tau_Q = 0.41 \times 10^{-11} x^{-(1/2)}$ sec from Van Kranendonk,[17] we find, for a concentration $x \simeq 10^{-2}$, that $W_{\text{eff}}^{D_2/D_2} = 1.32 \times 10^{-8}$ rad/sec for $J=1$ D_2 in $J=0$ D_2. The characteristic time for observing quantum-mechanical tunneling is therefore $W_{\text{eff}}^{-1} \simeq 3 \times 10^3$ h, which is much longer than the characteristic time if one only considers the magnetic interaction (angular momentum transfer), $R_{\text{mag}} \simeq 640$ h. The calculation of W_{eff} is, however, only accurate to an order of magnitude and we need a better test for tunneling than studies of $J=1$ D_2 in a $J=0$ D_2 matrix.

The interest in studying the diffusion of $J=1$ D_2 in a $J=0$ H_2 matrix is that angular momentum transfer is forbidden because of energy conservation considerations (a $J=1$ D_2 impurity at site i exchanging with a $J=0$ H_2 host molecule at site j requires $\Delta E \sim 85$ K).[24] Consequently, motion via zero point effects, quantum tunneling, is *the only possible mechanism* for diffusion. The diffusion of $J=1$ D_2 in $J=0$ H_2 is therefore a critical test of the tunneling motion *provided* the expected rates are measurable (i.e., longer than the natural conversion lifetimes of $J=1$ D_2 impurities in the host lattice).

For this scenario, we must again calculate two effects: (1) the basic microscopic tunneling frequency using general scaling arguments based on the MPEP approach, and (2) the effective reduction in the tunneling frequency due to the anisotropic EQQ interactions of the $J=1$ D_2 impurity.

The basic microscopic tunneling frequency is estimated by using as a starting point the inferred tunneling frequency of HD in a para-H_2 lattice. From experimental studies of the motional narrowing of HD impurities in solid para-H_2,[6,11-13] the tunneling frequency of HD in H_2 is accepted as $\omega^{HD/H_2} \sim 10^3$ Hz. Using this value for tunneling of HD in an H_2 matrix, we can estimate the tunneling for D_2 in an H_2 matrix by the following scaling ratio:

$$\frac{\ln\left[\frac{\omega^{D_2/H_2}}{\omega_0}\right]}{\ln\left[\frac{\omega^{HD/H_2}}{\omega_0}\right]} = \left[\frac{8}{7}\frac{V_{\text{eff}}(D_2/H_2)}{V_{\text{eff}}(HD/H_2)}\right]^{1/2} \frac{r_{D_2}}{r_{H_2}} , \tag{16}$$

where $\frac{8}{7}$ accounts for the mass effect, and r is the MPEP length. We will use a Lennard-Jones 6-12 potential for V_{eff} and, because the effective component of the potential which determines the tunneling (at closest approach) is the hard core, we have

$$\frac{V_{\text{eff}}(D_2/H_2)}{V_{\text{eff}}(HD/H_2)} \sim \left[\frac{r_{H_2}}{r_{D_2}}\right]^{12} . \tag{17}$$

Finally

$$\frac{\ln\left[\frac{\omega^{D_2/H_2}}{\omega_0}\right]}{\ln\left[\frac{\omega^{HD/H_2}}{\omega_0}\right]} = \left[\frac{8}{7}\right]^{1/2} \left[\frac{r_{H_2}}{r_{D_2}}\right]^5 . \tag{18}$$

Using $r_{H_2} = 1.18$ and $r_{D_2} = 1.145$,[25] as the estimates for the rms zero-point displacements, and $\omega_0 = 2.64 \times 10^{10}$ rad/sec (Ref. 18) as before, we find

$$\frac{\ln\left[\frac{\omega^{D_2/H_2}}{\omega_0}\right]}{\ln\left[\frac{\omega^{HD/H_2}}{\omega_0}\right]} = 1.24 , \tag{19}$$

which yields for the microscopic frequency

$$\omega^{D_2/H_2} = 162 \text{ rad/sec} . \tag{20}$$

The effective tunneling rate W_{eff} after accounting for the reduction due to the anisotropic EQQ and other interactions can then be determined by the following scaling:

$$W_{\text{eff}}^{D_2/H_2} = \left[\frac{\omega^{D_2/H_2}}{\omega^{D_2/D_2}}\right] W_{\text{eff}}^{D_2/D_2} \tag{21a}$$

$$= \left[\frac{162 \text{ rad/sec}}{11.3 \text{ rad/sec}}\right] 1.32 \times 10^{-8} \text{ rad/sec}$$

$$= 1.89 \times 10^{-7} \text{ rad/sec} = 3 \times 10^{-8} \text{ Hz} . \tag{21b}$$

If we use $r_{H_2}=1.134$ and $r_{D_2}=1.112$,[25] the same calculation as above yields $\omega^{D_2/H_2}=404$ rad/sec and thus

$$W_{\rm eff}^{D_2/H_2}=\left[\frac{404\ \text{rad/sec}}{11.3\ \text{rad/sec}}\right]1.32\times10^{-8}\ \text{rad/sec} \qquad (22a)$$

$$=4.71\times10^{-7}\ \text{rad/sec}=7.5\times10^{-8}\ \text{Hz}\ . \qquad (22b)$$

The MPEP approach to impurity tunneling therefore gives a range of values for the effective tunneling rates: $(3.0-7.5)\times10^{-8}$ Hz. In the following section we will compare this estimation with the experimental results of Ref. 15.

III. COMPARISON WITH EXPERIMENTAL RESULTS

In order to test for quantum tunneling in a case where the diffusion induced by the magnetic dipole-dipole interaction is forbidden, Krivchikov *et al.*[15] studied a sample with 0.94% paradeuterium ($J=1$) in a parahydrogen matrix (with 0.063% orthohydrogen). Angular momentum transfer by magnetic interactions between the dissimilar molecules H_2 and D_2 is forbidden because of the large change in rotational kinetic energy that would be required ($\Delta E=85.5$ K) compared to the strength of the weak magnetic interactions ($H\simeq10^{-5}$ K). As described previously, this would violate energy conservation. The diffusion of paradeuterium in parahydrogen must, therefore, proceed via the mass transfer mechanism only. Diffusion of HD molecules in parahydrogen can also only proceed by quantum tunneling, i.e., mass transfer, because in this case the impurity is always in the $J=0$ ground state.

Krivchikov *et al.*[15] studied the time dependence of the heat capacity peak of the $J=1$ D_2 molecules at a fixed low temperature. For isolated $J=1$ molecules in a very dilute random distribution in a sample prepared at time $t=0$, the contribution to the heat capacity is very small. At a later time t, as a result of quantum tunneling, the $J=1$ molecules will form small clusters (principally pairs and a small number of triplets) that are bound together in a low energy state as a result of their anisotropic electric quadrupole-quadrupole interactions. When thermal equilibrium is achieved, the resulting clusters have a Shottky-like heat capacity with a peak at $T\simeq1.75$ K (Fig. 4). Measurements of the time dependence of the heat capacity can therefore be used as an extremely sensitive probe for detecting very slow tunneling rates.

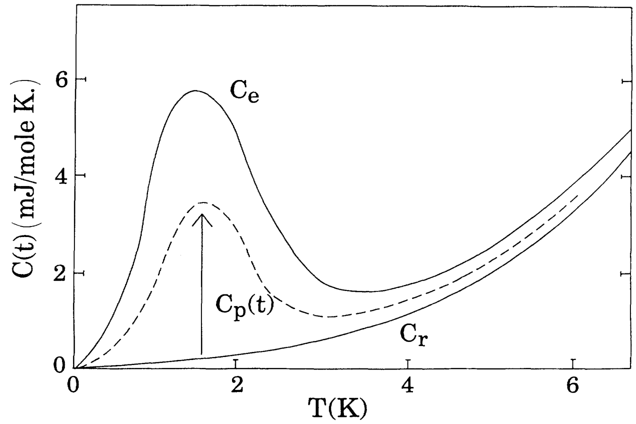

FIG. 4. Schematic representation of Shottky heat capacity peak C_e for an equilibrium distribution of ($J=1$) pairs in a ($J=0$) matrix. C_r is the heat capacity for an initially prepared sample with randomly distributed isolated molecules. $C_p(t)$ is the heat capacity observed at time t.

If C_e is the equilibrium heat capacity when all clusters are formed, and C_r is the heat capacity for the initial random distribution, the heat capacity $C_p(t)$ observed after aging for a time t is[16]

$$C_p(t)=C_e+(C_r-C_e)e^{-Wt}\ , \qquad (23)$$

where W is the effective clustering rate for quantum diffusion. The change in heat capacity recorded after time t is given by

$$\ln\left[\frac{C_e-C_p(t)}{C_e-C_r}\right]=-Wt\ . \qquad (24)$$

This is illustrated in Figs. 4 and 5. The heat capacity increases exponentially to the equilibrium value C_e, and for very slow rates, the initial slope is simply W (compare solid lines 1 and 2 of Fig. 5).

In Fig. 5 the observed time dependence of C_p is compared with the calculated variation for tunneling rates $W_{\rm eff}=10^{-2}$ h^{-1} (solid line 1) and 10^{-3} h^{-1} (solid line 2). The hatched region covers the range of $\Delta C(t)$ expected

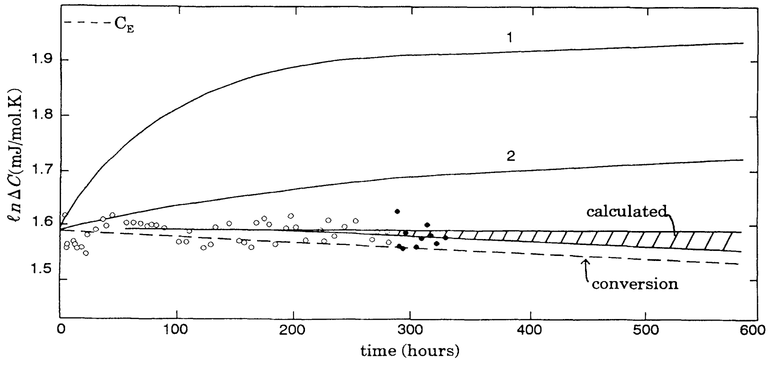

FIG. 5. Time dependence of heat capacity of a dilute solid mixture of para-D_2 ($x=0.94\%$) and ortho-H_2 ($x=0.064\%$) in a para-H_2 matrix. The circles are the data of Krivchikov *et al.* (Ref. 15), and the solid lines refer to the dependence calculated for tunneling rates $W_{\rm eff}=10^{-2}$ and 10^{-3} h^{-1}. The hatched region shows the dependencies predicted by the calculation reported here.

for our calculations of the effective tunneling rate $W_{\text{eff}}=(3.0\text{–}7.5)\times10^{-8}\ \text{s}^{-1}$. The comparison clearly shows that these experiments are not sufficiently sensitive to detect the theoretical tunneling rates. Consequently, the results of Krivchikov *et al.*[15] do not exclude quantum tunneling as described by the MPEP model given above.

The increase of the heat capacity with time due to quantum tunneling is offset by the "ordinary" $(J=1)$ to $(J=1)$ conversion driven by magnetic interactions. As the para-D_2 concentration decreases with conversion, the total heat capacity will also decrease. And indeed if the conversion rate was comparable to the tunneling rate, a net null result would be observed for the heat capacity studies. We therefore need to carefully estimate the conversion rate for the experiments of Krivchikov *et al.*[15] For the very dilute para-D_2 and ortho-H_2 concentrations in the samples studied, the para-D_2 conversion is given by[15]

$$\dot{x}(pD_2)=-\left[\frac{K_1}{12}M_1+\frac{K_2}{12}M_2\right]x(pD_2)\ , \tag{25}$$

where $K_1=4.8\times10^{-4}\ \text{h}^{-1}$ and $K_2=5.9\times10^{-3}\ \text{h}^{-1}$ are the conversion rates[26] for para-D_2–para-D_2 and para-D_2–ortho-H_2 clusters, respectively. M_1 and M_2 are the average numbers of the nearest-neighbor molecules to adjacent para-D_2 and ortho-H_2 molecules, respectively. For the concentrations of the two $(J=1)$ species in the sample, we find a net conversion rate

$$\dot{x}(pD_2)=-kx(pD_2)\ , \tag{26}$$

with $k=8.2\times10^{-6}\ \text{h}^{-1}$. The total number of para-D_2 molecules is $N^{pD_2}=N_s+2N_p+\cdots$, where N_s is the number of isolated singles and N_p is the number of pairs, and the conversion rate for pairs is $\dot{N}_p=2kN_p$. The *decrease* in the heat capacity due to conversion alone is therefore given by

$$C(t)|_{\text{conv}}=C(0)e^{-2kt}\ . \tag{27}$$

This is shown by the broken line in Fig. 5, and corresponds to $|\Delta C(t)/C|=5.6\times10^{-2}$. This is within the error bars of the measurements, but could be observed for experiments extended to longer time periods.

In view of the uncertainties in the calculation of the conversion rates,[26] Krivchikov *et al.*[15] carried out a careful comparison of the heat capacity of the aged sample with that of a freshly prepared random distribution for exactly the same concentration, by taking a sample aged 290 h and then quickly melting the sample and recrystallizing under the same conditions. Measurements of the heat capacity of the recrystallized sample (solid circles of Fig. 5) showed no significant difference from the values observed just before melting. Since the only difference between the samples is the thermal redistribution of the para-D_2 molecules, this null result shows that there is a negligible effect of pairing of para-D_2 in para-H_2 for $t\sim300$ h. Quantum tunneling, if present, would be limited to $W_{\text{eff}}<10^{-4}\ \text{h}^{-1}$. (This interpretation assumes that no back-conversion occurs when Krivchikov *et al.*[15] melted their sample. If the sample chamber contained a large amount of paramagnetic impurities on the walls, the back conversion in the liquid phase would then reset the sample concentration back to the values at $t=0$. The experimental conditions were carefully controlled to prevent this back-conversion.)

The most sensitive test of mass transfer by quantum tunneling, as opposed to angular momentum transfer by "resonant" conversion, is to date that of HD motion in solid para-H_2. The NMR measurements[6,7] are interpreted in terms of tunneling rates of $\sim10^3$ Hz, and in view of some of the uncertainties of the analysis of the NMR results we need a more stringent test for quantum tunneling. We propose a more direct test of quantum diffusion by using NMR stimulated echo techniques to detect the physical motion of HD molecules in an applied magnetic field gradient.

The stimulated echo observed in a $90°-\tau-90°-t-90°$ three-pulse sequence[27] is attenuated because of the dephasing of the spins as they move through a strong field gradient. This attenuation is given by

$$E(t)=E(0)\exp[-(\gamma^2D|\nabla B|^2\tau^2)t]\cdot e^{-t/T_1}e^{-2\tau/T_2}\ , \tag{28}$$

where the last two factors account for spin-lattice and spin-spin relaxation, respectively. For typical values of $\tau\sim T_2\sim10^{-3}$ s and $t\sim T_1\gtrsim10$ s, and a tunneling diffusion constant $D\simeq\frac{1}{3}Ja_0^2\sim10^{-12}\ \text{cm}^2\,\text{s}^{-1}$, the attenuation can be detected for field gradients $|\nabla B|\gtrsim10^4$ G cm^{-1}. This is achievable for practical designs for small volume gradient coils.

IV. CONCLUSIONS

We have used the method of the most probable escape path to calculate the tunneling of impurities in solid H_2 and D_2. In particular the tunneling of ortho-H_2 $(J=1)$ impurities in solid D_2 has been calculated and compared to the tunneling of $J=1$ H_2 and HD impurities in solid H_2. Comparison of these calculations with experiment provides an important test for the existence of quantum-mechanical tunneling due to particle exchange as opposed to that induced by magnetic interaction between the nuclear spins. Our calculations are consistent with the observations of the conversion of the molecular species in solid D_2 by Bagatskii *et al.*[16] We show that the tunneling of $J=1$ H_2 in solid D_2 is severely inhibited because of energy conservation, and the expected tunneling rates cannot be excluded by the recent experiments of Krivchikov *et al.*[15] The observations of the diffusion and line narrowing of HD impurities in solid H_2 give the strongest evidence obtained to date for particle-particle tunneling in solid H_2. We suggest a specific experiment to test for the tunneling by direct observation of particle-particle diffusion in an applied magnetic field gradient.

ACKNOWLEDGMENTS

We gratefully acknowledge many useful discussions with Horst Meyer, Paul Sokol, Pradeep Kumar, Valery Kokshenev, and Yasu Takano. The work was supported by a grant from the National Science Foundation, No. DMR 92 16785.

[1] R. A. Guyer, J. Low Temp. Phys. **8**, 427 (1972).

[2] R. A. Guyer, R. C. Richardson, and L. I. Zane, Rev. Mod. Phys. **45**, 532 (1971).

[3] J. M. Delrieu and N. S. Sullivan, Phys. Rev. B **23**, 3197 (1981).

[4] R. Oyarzun and J. Van Kranendonk, Can. J. Phys. **50**, 1494 (1972); R. A. Guyer and L. I. Zane, Phys. Rev. **188**, 445 (1969).

[5] D. Zhou, C. M. Edwards, and N. S. Sullivan, Phys. Rev. Lett. **62**, 1528 (1989).

[6] M. Rall, D. Zhou, E. G. Kisvarsanyi, and N. S. Sullivan, Phys. Rev. B **45**, 2800 (1992).

[7] E. G. Kisvarsanyi, K. Runge, and N. S. Sullivan, Phys. Lett. A **155**, 337 (1991).

[8] L. I. Amstutz, J. R. Thompson, and H. Meyer, J. Low Temp. Phys. **40**, 187 (1980).

[9] H. Meyer, Can. J. Phys. **65**, 1453 (1987).

[10] A. Farkas, *Orthohydrogen, Parahydrogen and Heavy Hydrogen* (Cambridge University Press, Cambridge, U.K., 1935).

[11] S. Washburn, R. Schweizer, and H. Meyer, J. Low Temp. Phys. **45**, 167 (1981).

[12] I. Yu, J. Low Temp. Phys. **60**, 425 (1985).

[13] E. G. Kisvarsanyi and N. S. Sullivan, Phys. Rev. B **46**, 2814 (1992).

[14] N. S. Sullivan, D. Zhou, M. Rall, and C. M. Edwards, Phys. Lett. A **138**, 329 (1989).

[15] A. I. Krivchikov, M. I. Bagatskii, V. G. Manzhelli, I. Ya Minchina, and P. I. Muromtsev, Sov. J. Low Temp. Phys. **15**, 1 (1989) [Fiz. Nizk. Temp. **15**, 3 (1989)].

[16] M. I. Bagatskii, A. I. Krivchikov, V. G. Manzhelli, I. Ya Minchina, and P. I. Muromtsev, Sov. J. Low Temp. Phys. **13**, 571 (1987) [Fiz. Nizk. Temp. **13**, 1001 (1987)].

[17] J. Van Kranendonk, *Solid Hydrogen* (Plenum, New York, 1983), Chap. 9.

[18] Erika G. Kisvarsanyi, M. S. thesis, University of Florida, 1990.

[19] C. G. Gray, Can. J. Phys. **54**, 505 (1976).

[20] F. H. Ree and C. F. Bender, J. Chem. Phys. **71**, 5362 (1979).

[21] J. Van Kranendonk, *Solid Hydrogen* (Ref. 17), Chap. 2.

[22] M. E. Rose, *Elementary Theory of Angular Momentum* (Wiley, New York, 1957).

[23] Y. Lin and N. S. Sullivan, J. Magn. Reson. **86**, 319 (1990).

[24] For a review of the properties of solid hydrogen, see I. F. Silvera, Rev. Mod. Phys. **52**, 393 (1980).

[25] M. Rall, M. S. thesis, University of Florida, 1988.

[26] M. A. Strzhemechnyi and O. I. Takar, Sov. J. Low Temp. Phys. **11**, 446 (1985) [Fiz. Nizk. Temp. **11**, 813 (1985)].

[27] J. E. Tanner, J. Chem. Phys. **52**, 2523 (1980).